

Article

Molecular Identification and Phylogenetic Analysis of *Cymbidium* Species (Orchidaceae) Based on the Potential DNA Barcodes *matK*, *rbcL*, *psbA-trnH*, and Internal Transcribed Spacer

Zhenming Chen ^{1,2,†}, Ling Gao ^{1,2,3,†}, Huizhong Wang ^{1,2} and Shangguo Feng ^{1,2,*}¹ College of Life and Environmental Sciences, Hangzhou Normal University, Hangzhou 311121, China² Zhejiang Provincial Key Laboratory for Genetic Improvement and Quality Control of Medicinal Plants, Hangzhou Normal University, Hangzhou 311121, China³ School of Basic Medicine, Hangzhou Normal University, Hangzhou 311121, China

* Correspondence: fengsg@hznu.edu.cn

† These authors have contributed equally to this work.

Abstract: Numerous *Cymbidium* species have significant commercial value globally due to their exotic ornamental flowers. Identifying *Cymbidium* species is challenging due to their similar shapes, which hinders their rational use and the conservation of germplasm resources. In the present study, firstly, four plastid loci (*matK*, *rbcL*, *psbA-trnH*, and *atpF-atpH*) and a nuclear locus (internal transcribed spacer, ITS) were initially examined to identify *Cymbidium* species. Secondly, we inferred the interspecific phylogeny of *Cymbidium* species using ITS sequences. All of these DNA regions, with the exception of *atpF-atpH*, could be readily amplified from *Cymbidium*, and the corresponding DNA sequences can be successfully obtained by sequencing. Our research demonstrated that ITS exhibited the highest intra- and interspecific divergences, the greatest barcoding gap, and the highest proportion of species identification. The phylogenetic analysis of *Cymbidium* species based on the ITS regions primarily corroborated the results obtained using traditional morphological methods. A comparative analysis of candidate DNA barcodes has shown that the ITS can be used not only for barcoding *Cymbidium* species but also for the phylogenetic analysis of *Cymbidium*.

Keywords: DNA barcoding; *Cymbidium*; species discrimination; phylogenetic study

Citation: Chen, Z.; Gao, L.; Wang, H.; Feng, S. Molecular Identification and Phylogenetic Analysis of *Cymbidium* Species (Orchidaceae) Based on the Potential DNA Barcodes *matK*, *rbcL*, *psbA-trnH*, and Internal Transcribed Spacer. *Agronomy* **2024**, *14*, 933.

<https://doi.org/10.3390/agronomy14050933>

Academic Editors: Nikolaos Nikoloudakis, Fengjie Sun and Angelos Kyrtziz

Received: 18 March 2024

Revised: 17 April 2024

Accepted: 27 April 2024

Published: 29 April 2024



Copyright: © 2024 by the authors. Licensee MDPI, Basel, Switzerland. This article is an open access article distributed under the terms and conditions of the Creative Commons Attribution (CC BY) license (<https://creativecommons.org/licenses/by/4.0/>).

1. Introduction

The genus *Cymbidium* Sw. (Orchidaceae) consists of 48–55 species and is primarily found in tropical and subtropical Asia, as well as northern and eastern Australia [1]. *Cymbidium* orchids are well known in worldwide horticulture due to their variegated leaves and fragrant flowers, and they have been cultivated for more than ten centuries [2,3]. Due to their significant economic value, large quantities of *Cymbidium* species were harvested and traded in China. In recent years, natural *Cymbidium* populations have faced a serious threat of extinction due to overcollection and habitat destruction. All *Cymbidium* species are included in the Convention on International Trade in Endangered Species of Wild Fauna and Flora (CITES).

The unequivocal identification and examination of the phylogenetic relationships of *Cymbidium* plants are essential for sustainable conservation and increased utilization. Traditionally, *Cymbidium* species' identification and plant phylogeny assessment were primarily conducted through morphological [4] and anatomical analyses [5]. Schlechter (1924) suggests a system for categorizing *Cymbidium* into eight sections, which forms the foundation of the current infrageneric classification of *Cymbidium* [6]. Most of these sections are still acknowledged in their original form to some extent. Hunt (1970) incorporated *Cyperorchis* into *Cymbidium* and upheld Schlechter's sectional classifications [7]. Seth and Cribb (1984) initially categorized *Cymbidium* into three subgenera: subgenus *Cymbidium*,

subgenus *Cyperorchis*, and subgenus *Jensoa* [8]. Later, further supplementary studies and improvement in the classification of the genus were conducted by Puy and Cribb (1988) [9] and Liu et al. (2006) [10]. However, morphological and anatomical characteristics are easily influenced by the environmental conditions of plant growth, and it is occasionally challenging to distinguish *Cymbidium* species based solely on these characteristics [3,11,12]. Consequently, a simple and accurate identification of *Cymbidium* species is essential.

DNA barcoding is a method of molecular identification that uses brief, standardized DNA sequences to rapidly determine the species of specimens [13–16]. The mitochondrial cytochrome *c oxidase 1* gene (*COI*) has been widely accepted as a universal barcode for species identification in many animal groups [17–19]. Several regions of chloroplast DNA sequences, such as *matK*, *rbcL*, *rpoB*, *rpoC1*, *psbA-trnH*, and *atpF-atpH* spacers, as well as the internal transcribed spacer (ITS) region of the nuclear ribosomal DNA, have been proposed as potential plant barcodes [20–22]. To this day, a universally recognized barcode for plants has yet to be established [21,23]. Four DNA regions—*matK*, *rpoB*, *rpoC1*, and *trnH-psbA*—were analyzed to discriminate *Cymbidium* species in Thailand [24]. The phylogenetic relationships of *Cymbidium* have been preliminarily analyzed using various molecular markers, including RAPD [25], AFLP [26], ISSR [27,28], and SSR [29]. The *matK* and ITS regions were also employed for assessing the phylogenetic relationships among several *Cymbidium* species [30,31]. Furthermore, previous studies have suggested that the complete chloroplast genome can serve as an effective tool for identifying *Cymbidium* species and resolving their phylogenetic relationships [1,32,33]. Although there has been progress in these studies, the genetic relationships between many species of *Cymbidium* remain controversial [31,34,35]. Therefore, further study is needed using more efficient molecular techniques for *Cymbidium* species.

Our study aimed at (1) testing the universality of a set of DNA regions in *Cymbidium*, (2) evaluating the potential of these barcodes for identifying *Cymbidium* species, and (3) reconstructing the phylogenetic relationships within the genus *Cymbidium*. We compared the potential of using five different DNA barcodes (ITS, *matK*, *rbcL*, *psbA-trnH*, and *atpF-atpH*) and four combinations of regions (ITS + *matK*, ITS + *psbA-trnH*, ITS + *matK* + *psbA-trnH*, and *matK* + *rbcL*) for the identification of *Cymbidium* species. The best DNA barcode sequences were then chosen as genetic markers to analyze the phylogenetic relationships among 29 *Cymbidium* species.

2. Materials and Methods

2.1. Plant Materials

We collected as many *Cymbidium* species as possible, and 34 individuals from 18 species were used to assess the success rate of PCR amplification and sequencing. Due to the valuable, rare, and challenging nature of *Cymbidium* plants, the sample size for each *Cymbidium* species in this study varied from 1 to 4, with 6 species represented by 2 or more individuals. The specimens were obtained from the primary distribution regions of orchids in China. The species and voucher specimens collected are detailed in Table S1. The samples originated from nine provinces: Yunnan, Zhejiang, Guangdong, Guangxi, Jiangxi, Henan, Fujian, Anhui, and Guizhou. In this study, 34 *Cymbidium* samples were sequenced, resulting in a total of 136 sequences, comprising 34 ITS, 34 *matK*, 34 *psbA-trnH*, and 34 *rbcL* sequences, respectively (Table S2). Other published ITS sequences for 20 *Cymbidium* species were downloaded from GenBank for further phylogenetic analysis (Table S3). All pertinent studies involving the gathered samples received approval from Hangzhou Normal University.

2.2. DNA Extraction, Amplification, and Sequencing

We utilized the Plant Genomic DNA Kit (Sangon Co., Shanghai, China) to extract genomic DNA from fresh young leaves following the provided protocol. The nuclear DNA ITS and four chloroplast genome regions, including two coding genes (*matK* and *rbcL*) and two intergenic spacer sequences (*psbA-trnH* and *atpF-atpH*), were amplified using the

specified primer pairs and reaction procedures outlined in Table 1. The PTC-100 thermal cycler (MJ Research, Waltham, MA, USA) was utilized for the amplification process. The purified PCR products were sequenced in both directions using the primers employed for PCR amplification by Shanghai Sunny Biotechnology Co. Ltd. (Shanghai, China). Since the sequencing was unsuccessful, the *atpF-atpH* region was excluded from further analysis (see results).

Table 1. PCR primers and reaction procedures of five DNA regions.

DNA Region	Primer Name	Sequence (5'-3')	Amplification Protocol
ITS	ITS4	TCCTCCGCTTATTGATATGC	94 °C 5 min; 94 °C 1 min, 55 °C 1 min;
	ITS5	GGAAGGAGAAGTCGTAACAAGG	72 °C 1.5 min, 35 cycles; 72 °C 10 min
<i>matK</i>	<i>matK-1F</i>	CGTACAGTACTTTTGTGTTACGAG	94 °C 5 min; 94 °C 1 min, 60 °C 1 min;
	<i>matK-1R</i>	ACCCAGTCCATCTGGAATCTTGGTTC	72 °C 1.5 min, 30 cycles; 72 °C 10 min
<i>rbcL</i>	<i>rbcL-1F</i>	ATGTCACCACAAACAGAGACTAAAGC	95 °C 2 min; 94 °C 1 min, 55 °C 1 min;
	<i>rbcL-1R</i>	GTAAAATCAAGTCCACCRCG	72 °C 1.5 min, 35 cycles; 72 °C 10 min
<i>psbA-trnH</i>	<i>psbA-3F</i>	GTTATGCATGAACGTAATGCTC	94 °C 5 min; 94 °C 1 min, 55 °C 1 min;
	<i>trnHF</i>	CGCGCATGGTGGATTACAATCC	72 °C 1.5 min, 32 cycles; 72 °C 10 min
<i>atpF-atpH</i>	<i>atpF-H/f</i>	ACTCGCACACTCCCTTTCC	94 °C 5 min; 94 °C 1 min, 50 °C 1 min;
	<i>atpF-H/R</i>	GCTTTTATGGAAGCTTTAACAAT	72 °C 1.5 min, 35 cycles; 72 °C 10 min

2.3. Data Analysis

The assembly of contigs and the generation of consensus sequences were performed using CodonCode Aligner V3.0 (CodonCode Co., Centerville, MA, USA) following established protocols. The DNA barcode candidate sequences, including ITS, *matK*, *rbcL*, and *psbA-trnH*, as well as combinations of these regions (ITS + *matK*, ITS + *psbA-trnH*, ITS + *matK* + *psbA-trnH*, and *matK* + *rbcL*), were aligned using the Clustal W 2.1 software (Informer Technologies, Inc., Los Angeles, CA, USA) [36]. The genetic distances were calculated in MEGA 7.0 using the Kimura 2-Parameter (K2P) model [37]. The dataset was thoroughly reviewed and any positions with gaps or missing data were excluded. The K2P model was utilized to quantify interspecific divergences, with the average and minimum interspecific distances as well as Theta prime serving as representative measures [21,38]. Intraspecific variation was assessed through the calculation of average intraspecific distance, coalescent depth, and theta [21,38]. We compared the differences in variability within and between species by analyzing DNA barcoding gaps [21,38]. Paired Wilcoxon signed-rank tests were conducted as previously described [21]. To further assess the efficacy of barcoding candidates for species identification, we employed the nearest distance method as previously described [21]. The discriminatory ability of barcoding candidates for sister species was assessed using TaxonGap 2.4.1 software [39]. The secondary structure of the ITS2 region of the ITS sequence was predicted according to the ITS2 database (<https://its2.bioapps.biozentrum.uni-wuerzburg.de/>, accessed on 15 December 2023).

All *Cymbidium* species included in our study (Tables S1 and S3) were categorized into three subgenera: *Cymbidium*, *Cyperorchis*, and *Jensoa* [8,40]. These included nine sections (sect.): *Cymbidium* Lindl, *Himentophyllum* Schltr, *Floribunda* Seth et Cribb, *Iridorchis* (Bl.) P. F., *Eburnea* Seth et Cribb, *Cyperorchis* (Bl.) P. F., *Parishiella* (Schltr.) P. F., *Jensoa* (Rafin.) Schltr., and *Geocymbidium* Schltr. The maximum likelihood (ML) method in MEGA 7.0 was utilized to build the phylogenetic tree [37]. For ML analysis, we utilized the Tamura-Nei model as the best model. The bootstrap support (BS) values for particular clades were calculated by running 1000 bootstrap replicates of the dataset. Four *Pholidota* species were used as outgroups: *P. bulbocodioides*, *P. praecox*, *P. formosana*, and *P. albiflora*. The GenBank accession numbers of their ITS sequences are AF302739, JN114695, AF302740, and AY101967, respectively.

3. Results

3.1. PCR Amplification Success Rate and Sequence Characteristics

The PCR amplification and sequencing success rates for ITS, *matK*, *rbcL*, and *psbA-trnH* sequences were all 100%. However, the *atpF-atpH* sequence could not be successfully amplified and sequenced; so, it was excluded from subsequent analyses. The accession numbers for GenBank can be found in Table S2. The lengths of the ITS and *psbA-trnH* sequences showed significant variation across different *Cymbidium* species, whereas the coding regions, such as *matK* and *rbcL*, exhibited a relatively consistent length. The ITS had the highest proportion of variable nucleotides at 11.2%, while the *rbcL* had the lowest at 5.0%. ITS showed the highest mean GC content (68.4%), followed by *rbcL* (42.9%) and *psbA-trnH* (34.0%); meanwhile, *matK* had the lowest mean GC ratio (32.1%) (Table 2).

Table 2. Evaluation of five DNA regions and combinations of the regions.

	No. of Samples/Species	PCR Success (%)	Sequencing Success (%)	Aligned Length (bp)	N Variable Characters (%Variable Characters)	G+C Ratio (%)	Ability to Discriminate
ITS	34/18	100	100	661	74 (11.2)	68.4	93.20%
<i>matK</i>	34/18	100	100	848	59 (7.0)	32.1	75.80%
<i>psbA-trnH</i>	34/18	100	100	845	87 (10.3)	34	87.10%
<i>rbcL</i>	34/18	100	100	575	28 (5.0)	42.9	54.20%
<i>atpF-atpH</i>	34/18	low	low	-	-	-	-
ITS + <i>matK</i>	34/18	-	-	1509	131 (8.7)	47.9	88.50%
ITS + <i>psbA-trnH</i>	34/18	-	-	1510	159 (10.5)	50	90.90%
ITS + <i>matK</i> + <i>psbA-trnH</i>	34/18	-	-	2362	213 (9.0)	42.1	93.20%
<i>matK</i> + <i>rbcL</i>	34/18	-	-	1686	162 (9.6)	33	67.00%

3.2. Genetic Divergence within and between Species

ITS exhibited significantly higher divergence compared to *matK*, *psbA-trnH*, and the combinations of regions (ITS + *matK*, ITS + *psbA-trnH*, ITS + *matK* + *psbA-trnH*, and *matK* + *rbcL*) at the interspecific level (Figures 1 and 2). The *rbcL* region showed the lowest divergence in all interspecific calculations, while the ITS region exhibited the highest level of divergence at the interspecific level, as confirmed by Wilcoxon signed-rank tests (Table 3). At the intraspecific level, the lowest divergence was for *psbA-trnH* (Figures 1 and 2). Comparable results were achieved when employing Wilcoxon signed-rank tests (Table 4).

Table 3. Wilcoxon signed-rank tests of interspecific divergence among loci.

W+	W-	Relative Ranks, n, p Value	Result
ITS	<i>matK</i>	W+ = 122,851.5, W- = 12,088.5, n = 519, p ≤ 5.144 × 10 ⁻⁵⁹	ITS > <i>matK</i>
ITS	<i>psbA-trnH</i>	W+ = 119,137, W- = 8123, n = 504, p ≤ 1.492 × 10 ⁻⁶⁴	ITS > <i>psbA-trnH</i>
ITS	<i>rbcL</i>	W+ = 126,189, W- = 2082, n = 506, p ≤ 2.735 × 10 ⁻⁷⁹	ITS > <i>rbcL</i>
ITS	ITS + <i>matK</i>	W+ = 124,066.5, W- = 7774.5, n = 513, p ≤ 4.208 × 10 ⁻⁶⁷	ITS > ITS + <i>matK</i>
ITS	ITS + <i>psbA-trnH</i>	W+ = 127,702.5, W- = 3113.5, n = 511, p ≤ 1.259 × 10 ⁻⁷⁷	ITS > ITS + <i>psbA-trnH</i>
ITS	ITS + <i>matK</i> + <i>psbA-trnH</i>	W+ = 122,080, W- = 4173, n = 502, p ≤ 1.982 × 10 ⁻⁷³	ITS > ITS + <i>matK</i> + <i>psbA-trnH</i>
ITS	<i>matK</i> + <i>rbcL</i>	W+ = 129,347, W- = 4039, n = 516, p ≤ 2.675 × 10 ⁻⁷⁶	ITS > <i>matK</i> + <i>rbcL</i>
<i>matK</i>	<i>psbA-trnH</i>	W+ = 71,961, W- = 55,804, n = 505, p ≤ 0.01381	<i>matK</i> > <i>psbA-trnH</i>
<i>matK</i>	<i>rbcL</i>	W+ = 107,518, W- = 18,233, n = 501, p ≤ 4.034 × 10 ⁻⁴³	<i>matK</i> > <i>rbcL</i>
<i>matK</i>	ITS + <i>matK</i>	W+ = 20,587.5, W- = 103,663.5, n = 498, p ≤ 3.24 × 10 ⁻³⁸	<i>matK</i> < ITS + <i>matK</i>
<i>matK</i>	ITS + <i>psbA-trnH</i>	W+ = 33,000.5, W- = 93,755.5, n = 503, p ≤ 1.251 × 10 ⁻²⁰	<i>matK</i> < ITS + <i>psbA-trnH</i>
<i>matK</i>	ITS + <i>matK</i> + <i>psbA-trnH</i>	W+ = 37,713, W- = 87,037, n = 499, p ≤ 1.988 × 10 ⁻¹⁴	<i>matK</i> < ITS + <i>matK</i> + <i>psbA-trnH</i>

Table 3. Cont.

W+	W−	Relative Ranks, <i>n</i> , <i>p</i> Value	Result
<i>matK</i>	<i>matK + rbcL</i>	W+ = 76,946, W− = 30,007, <i>n</i> = 462, <i>p</i> ≤ 3.024 × 10 ^{−16}	<i>matK</i> > <i>matK + rbcL</i>
<i>psbA-trnH</i>	<i>rbcL</i>	W+ = 80,886, W− = 15,255, <i>n</i> = 438, <i>p</i> ≤ 3.479 × 10 ^{−35}	<i>psbA-trnH</i> > <i>rbcL</i>
<i>psbA-trnH</i>	<i>ITS + matK</i>	W+ = 25,876.5, W− = 106,993.5, <i>n</i> = 515, <i>p</i> ≤ 3.492 × 10 ^{−33}	<i>psbA-trnH</i> < <i>ITS + matK</i>
<i>psbA-trnH</i>	<i>ITS + psbA-trnH</i>	W+ = 22,874, W− = 100,879, <i>n</i> = 497, <i>p</i> ≤ 4.331 × 10 ^{−34}	<i>psbA-trnH</i> < <i>ITS + psbA-trnH</i>
<i>psbA-trnH</i>	<i>ITS + matK + psbA-trnH</i>	W+ = 35,329.5, W− = 93,448.5, <i>n</i> = 507, <i>p</i> ≤ 1.329 × 10 ^{−18}	<i>psbA-trnH</i> < <i>ITS + matK + psbA-trnH</i>
<i>psbA-trnH</i>	<i>matK + rbcL</i>	W+ = 70,183.5, W− = 56,069.5, <i>n</i> = 502, <i>p</i> ≤ 0.03	<i>psbA-trnH</i> > <i>matK + rbcL</i>
<i>rbcL</i>	<i>ITS + matK</i>	W+ = 7126, W− = 129,900, <i>n</i> = 523, <i>p</i> ≤ 1.721 × 10 ^{−70}	<i>rbcL</i> < <i>ITS + matK</i>
<i>rbcL</i>	<i>ITS + psbA-trnH</i>	W+ = 4827.5, W− = 120,422.5, <i>n</i> = 500, <i>p</i> ≤ 1.772 × 10 ^{−71}	<i>rbcL</i> < <i>ITS + psbA-trnH</i>
<i>rbcL</i>	<i>ITS + matK + psbA-trnH</i>	W+ = 11,060, W− = 121,810, <i>n</i> = 515, <i>p</i> ≤ 2.417 × 10 ^{−60}	<i>rbcL</i> < <i>ITS + matK + psbA-trnH</i>
<i>rbcL</i>	<i>matK + rbcL</i>	W+ = 16,738.5, W− = 102,089.5, <i>n</i> = 487, <i>p</i> ≤ 6.601 × 10 ^{−43}	<i>rbcL</i> < <i>matK + rbcL</i>
<i>ITS + matK</i>	<i>ITS + psbA-trnH</i>	W+ = 69,846, W− = 40,369, <i>n</i> = 469, <i>p</i> ≤ 5.215 × 10 ^{−7}	<i>ITS + matK</i> > <i>ITS + psbA-trnH</i>
<i>ITS + matK</i>	<i>ITS + matK + psbA-trnH</i>	W+ = 112,461.5, W− = 5879.5, <i>n</i> = 486, <i>p</i> ≤ 2.658 × 10 ^{−66}	<i>ITS + matK</i> > <i>ITS + matK + psbA-trnH</i>
<i>ITS + matK</i>	<i>matK + rbcL</i>	W+ = 117,120.5, W− = 2195.5, <i>n</i> = 488, <i>p</i> ≤ 7.187 × 10 ^{−76}	<i>ITS + matK</i> > <i>matK + rbcL</i>
<i>ITS + psbA-trnH</i>	<i>matK + psbA-trnH</i>	W+ = 118,283, W− = 9988, <i>n</i> = 506, <i>p</i> ≤ 8.182 × 10 ^{−61}	<i>ITS + psbA-trnH</i> > <i>matK + psbA-trnH</i>
<i>ITS + psbA-trnH</i>	<i>matK + rbcL</i>	W+ = 118,735.5, W− = 8020.5, <i>n</i> = 503, <i>p</i> ≤ 1.376 × 10 ^{−64}	<i>ITS + psbA-trnH</i> > <i>matK + rbcL</i>
<i>ITS + matK + psbA-trnH</i>	<i>matK + rbcL</i>	W+ = 115,863, W− = 6402, <i>n</i> = 494, <i>p</i> ≤ 1.386 × 10 ^{−66}	<i>ITS + matK + psbA-trnH</i> > <i>matK + rbcL</i>

Table 4. Wilcoxon signed-rank tests of intraspecific divergence among loci.

W+	W−	Relative Ranks, <i>n</i> , <i>p</i> Value	Result
<i>ITS</i>	<i>matK</i>	W+ = 161, W− = 217, <i>n</i> = 27, <i>p</i> ≤ 0.5088	<i>ITS</i> = <i>matK</i>
<i>ITS</i>	<i>psbA-trnH</i>	W+ = 225, W− = 51, <i>n</i> = 23, <i>p</i> ≤ 0.008516	<i>ITS</i> > <i>psbA-trnH</i>
<i>ITS</i>	<i>rbcL</i>	W+ = 182, W− = 94, <i>n</i> = 23, <i>p</i> ≤ 0.1858	<i>ITS</i> = <i>rbcL</i>
<i>ITS</i>	<i>ITS + matK</i>	W+ = 161, W− = 217, <i>n</i> = 27, <i>p</i> ≤ 0.5088	<i>ITS</i> = <i>ITS + matK</i>
<i>ITS</i>	<i>ITS + psbA-trnH</i>	W+ = 225, W− = 51, <i>n</i> = 23, <i>p</i> ≤ 0.008516	<i>ITS</i> > <i>ITS + psbA-trnH</i>
<i>ITS</i>	<i>ITS + matK + psbA-trnH</i>	W+ = 151, W− = 102, <i>n</i> = 22, <i>p</i> ≤ 0.4359	<i>ITS</i> = <i>ITS + matK + psbA-trnH</i>
<i>ITS</i>	<i>matK + rbcL</i>	W+ = 169, W− = 209, <i>n</i> = 27, <i>p</i> ≤ 0.6394	<i>ITS</i> = <i>matK + rbcL</i>
<i>matK</i>	<i>psbA-trnH</i>	W+ = 231, W− = 0, <i>n</i> = 21, <i>p</i> ≤ 6.414 × 10 ^{−5}	<i>matK</i> > <i>psbA-trnH</i>
<i>matK</i>	<i>rbcL</i>	W+ = 191, W− = 62, <i>n</i> = 22, <i>p</i> ≤ 0.03773	<i>matK</i> > <i>rbcL</i>
<i>matK</i>	<i>ITS + matK</i>	W+ = 186, W− = 67, <i>n</i> = 22, <i>p</i> ≤ 0.05543	<i>matK</i> = <i>ITS + matK</i>
<i>matK</i>	<i>ITS + psbA-trnH</i>	W+ = 228.5, W− = 47.5, <i>n</i> = 23, <i>p</i> ≤ 0.006194	<i>matK</i> > <i>ITS + psbA-trnH</i>
<i>matK</i>	<i>ITS + matK + psbA-trnH</i>	W+ = 192.5, W− = 17.5, <i>n</i> = 20, <i>p</i> ≤ 0	<i>matK</i> > <i>ITS + matK + psbA-trnH</i>
<i>matK</i>	<i>matK + rbcL</i>	W+ = 111.5, W− = 24.5, <i>n</i> = 16, <i>p</i> ≤ 0	<i>matK</i> > <i>matK + rbcL</i>
<i>psbA-trnH</i>	<i>rbcL</i>	W+ = 3.5, W− = 51.5, <i>n</i> = 10, <i>p</i> ≤ 0	<i>psbA-trnH</i> < <i>rbcL</i>
<i>psbA-trnH</i>	<i>ITS + matK</i>	W+ = 13, W− = 393, <i>n</i> = 28, <i>p</i> ≤ 1.596 × 10 ^{−5}	<i>psbA-trnH</i> < <i>ITS + matK</i>
<i>psbA-trnH</i>	<i>ITS + psbA-trnH</i>	W+ = 36, W− = 264, <i>n</i> = 24, <i>p</i> ≤ 0.001183	<i>psbA-trnH</i> < <i>ITS + psbA-trnH</i>
<i>psbA-trnH</i>	<i>ITS + matK + psbA-trnH</i>	W+ = 18, W− = 333, <i>n</i> = 26, <i>p</i> ≤ 6.681 × 10 ^{−5}	<i>psbA-trnH</i> < <i>ITS + matK + psbA-trnH</i>
<i>psbA-trnH</i>	<i>matK + rbcL</i>	W+ = 0, W− = 276, <i>n</i> = 23, <i>p</i> ≤ 2.891 × 10 ^{−5}	<i>psbA-trnH</i> < <i>matK + rbcL</i>
<i>rbcL</i>	<i>ITS + matK</i>	W+ = 134.5, W− = 330.5, <i>n</i> = 30, <i>p</i> ≤ 0.04492	<i>rbcL</i> < <i>ITS + matK</i>
<i>rbcL</i>	<i>ITS + psbA-trnH</i>	W+ = 150, W− = 175, <i>n</i> = 25, <i>p</i> ≤ 0.7468	<i>rbcL</i> = <i>ITS + psbA-trnH</i>
<i>rbcL</i>	<i>ITS + matK + psbA-trnH</i>	W+ = 148.5, W− = 229.5, <i>n</i> = 27, <i>p</i> ≤ 0.3366	<i>rbcL</i> = <i>ITS + matK + psbA-trnH</i>
<i>rbcL</i>	<i>matK + rbcL</i>	W+ = 59.5, W− = 193.5, <i>n</i> = 22, <i>p</i> ≤ 0.03085	<i>rbcL</i> < <i>matK + rbcL</i>
<i>ITS + matK</i>	<i>ITS + psbA-trnH</i>	W+ = 128.5, W− = 7.5, <i>n</i> = 16, <i>p</i> ≤ 0	<i>ITS + matK</i> > <i>ITS + psbA-trnH</i>
<i>ITS + matK</i>	<i>ITS + matK + psbA-trnH</i>	W+ = 171, W− = 0, <i>n</i> = 18, <i>p</i> ≤ 0	<i>ITS + matK</i> > <i>ITS + matK + psbA-trnH</i>
<i>ITS + matK</i>	<i>matK + rbcL</i>	W+ = 114, W− = 96, <i>n</i> = 20, <i>p</i> ≤ 0	<i>ITS + matK</i> > <i>matK + rbcL</i>
<i>ITS + psbA-trnH</i>	<i>ITS + matK + psbA-trnH</i>	W+ = 72, W− = 138, <i>n</i> = 20, <i>p</i> ≤ 0	<i>ITS + psbA-trnH</i> < <i>ITS + matK + psbA-trnH</i>
<i>ITS + psbA-trnH</i>	<i>matK + rbcL</i>	W+ = 76, W− = 224, <i>n</i> = 24, <i>p</i> ≤ 0.03573	<i>ITS + psbA-trnH</i> < <i>matK + rbcL</i>
<i>ITS + matK + psbA-trnH</i>	<i>matK + rbcL</i>	W+ = 30, W− = 141, <i>n</i> = 18, <i>p</i> ≤ 0	<i>ITS + matK + psbA-trnH</i> < <i>matK + rbcL</i>

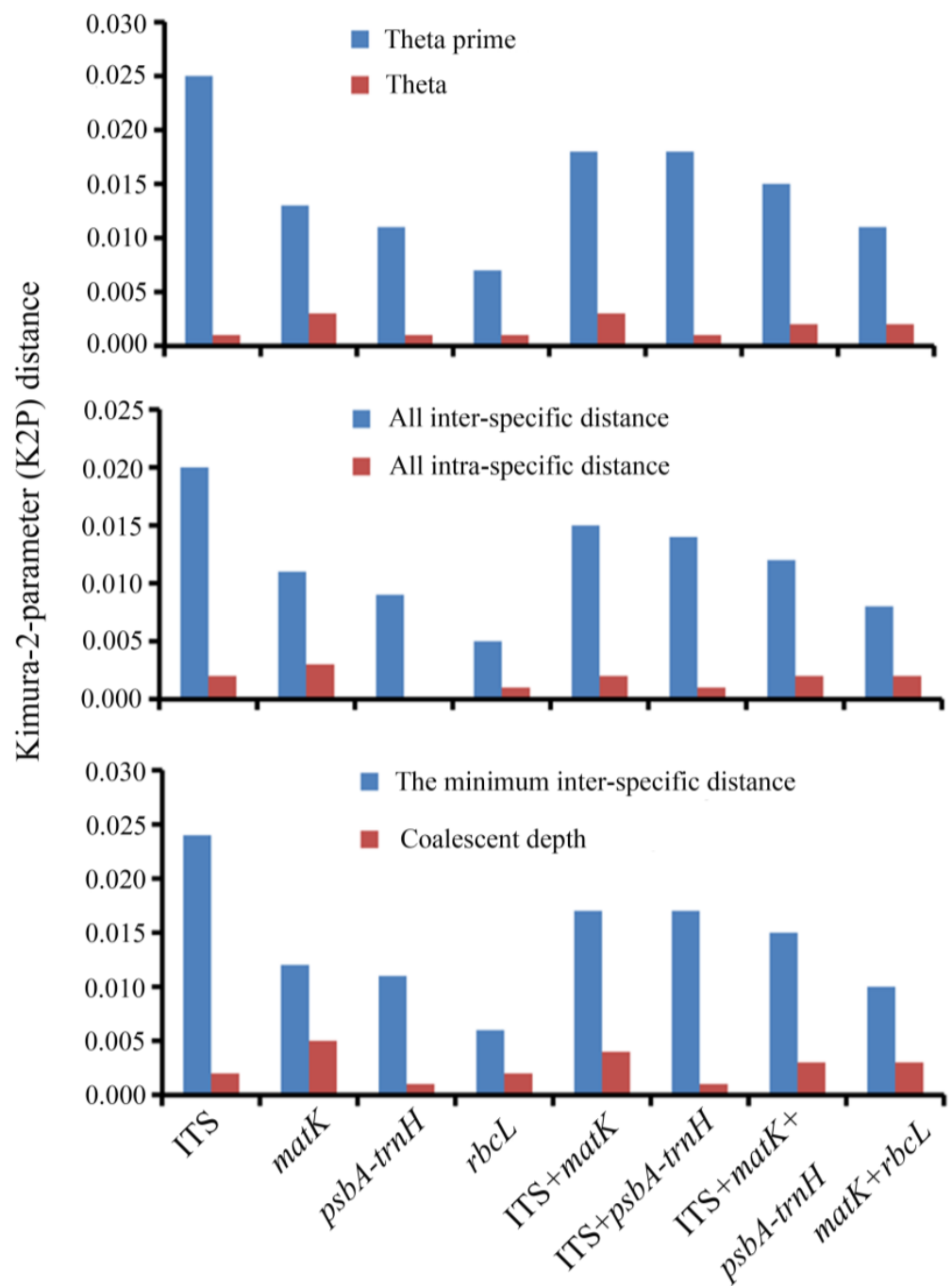


Figure 1. Analyses of intra- and interspecific divergence of four loci and four regional combinations based on six metrics.

3.3. Assessment of the Barcoding Gap

No discrepancies in barcoding were observed in any of the four potential loci or their combinations. Compared to *matK*, *psbA-trnH*, and *rbcL*, ITS exhibited only a slight difference in both inter- and intraspecific variation (Figure 3). In terms of the combined regions, the variations in ITS + *psbA-trnH* were the most significant, while the overlap in *matK* + *rbcL* was the largest (Figure 3).

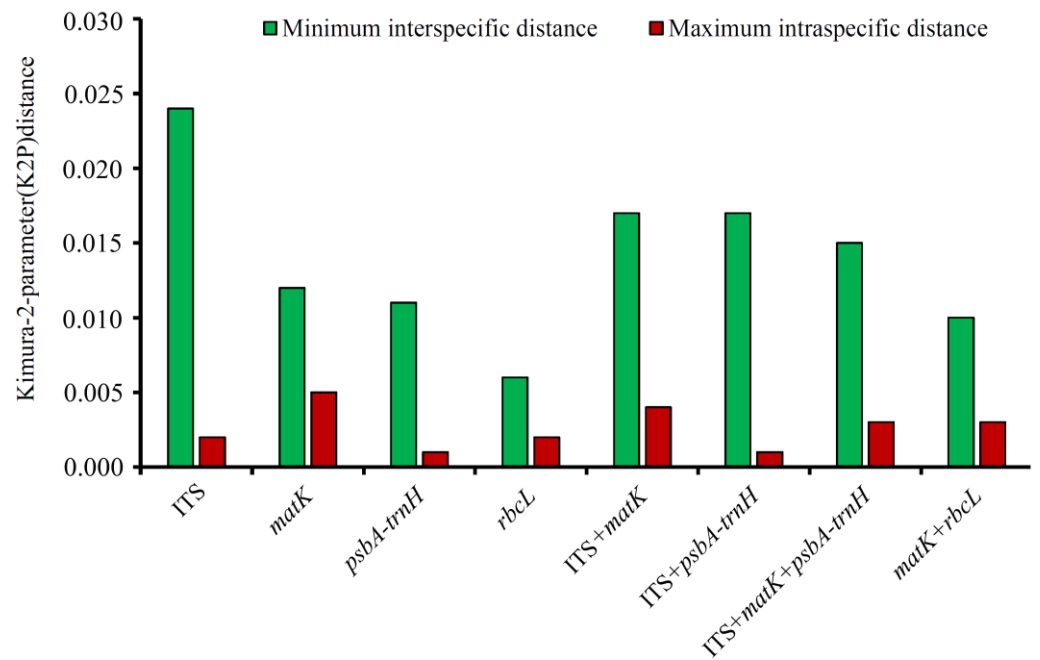


Figure 2. Analyses of the minimum interspecific distance and the maximum intraspecific distance of four loci and four regional combinations.

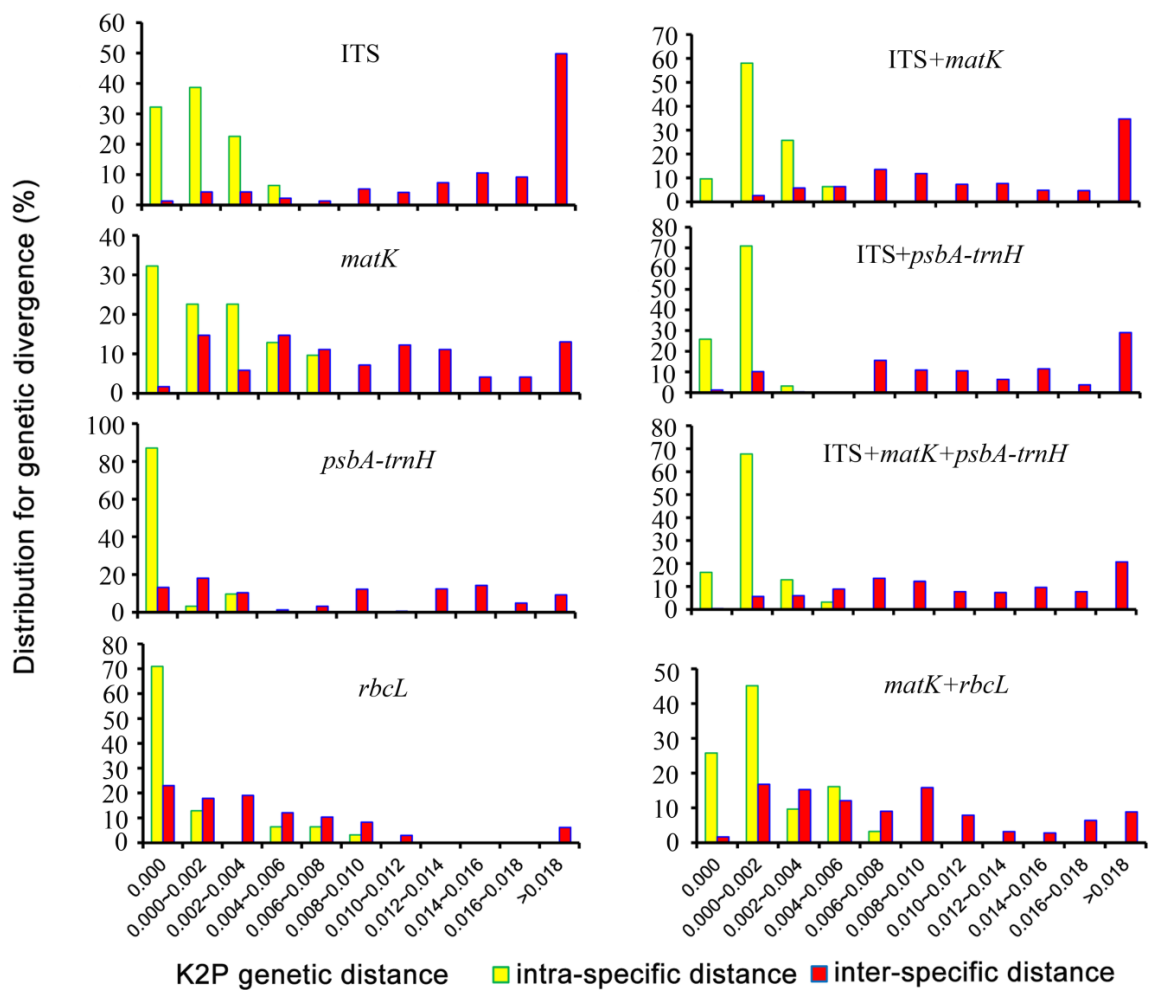


Figure 3. Distribution of the intra- and interspecific variations of the four loci and four regional combinations in *Cymbidium* species.

3.4. Applicability for Species Authentication

Among the four candidate loci, ITS provided 93.2% species resolution, followed by *matK* with 75.8%, *rbcL* with 54.2%, and *psbA-trnH* with 87.1%. The species identification rates for the combined regions were 88.5%, 90.9%, 93.2%, and 67.0% for ITS + *matK*, ITS + *psbA-trnH*, ITS + *matK* + *psbA-trnH*, and *matK* + *rbcL*, respectively (Table 2). The ITS method was simpler and more cost-effective, even though both the ITS sequences and the combination of ITS + *matK* + *psbA-trnH* yielded the same species resolution.

3.5. Evaluation of the Discriminatory Power of Candidate Barcoding

The ability of barcoding to distinguish potential sister species in gathered samples was assessed (Figures 4 and 5). The interspecific diversity was greater than the intraspecific diversity for more than 72.2% of species in ITS sequences and the combined regions of ITS + *matK*, ITS + *psbA-trnH*, and ITS + *matK* + *psbA-trnH*. The percentage of species with greater interspecific diversity than intraspecific diversity in the remaining loci were 61.1%, 50.0%, 33.0%, and 66.7% for *matK*, *psbA-trnH*, *rbcL*, and *matK* + *rbcL*, respectively. The results also showed that ITS could be a powerful tool for distinguishing the tested *Cymbidium* species. However, even for ITS sequences, there were still some cases, 22.2% of the species (as shown by the dark gray bar in Figures 4 and 5), that had almost identical sequences with their sister species for *C. georingii* compared to *C. georingii* var. *longibracteatum* and *C. kanran* compared to *C. sinense*.

3.6. Analysis of ITS2 Secondary Structure

The secondary structure of the ITS2 regions within the ITS sequences were analyzed for species differentiation between closely related species, specifically *C. georingii* and *C. georingii* var. *longibracteatum*, as well as *C. kanran* and *C. sinense*. All species share a similar secondary structure consisting of four stem-loops, labeled as I, II, III, and IV. The ITS2 secondary structure can be used to directly distinguish between *C. kanran* and *C. sinense*. Although the secondary structures of *C. georingii* and *C. georingii* var. *longibracteatum* are highly conserved in stem-loops II, III, and IV, some differences in stem-loop I can be utilized for species differentiation (Figure 6).

3.7. Phylogenetic Analysis

The maximum likelihood phylogenetic tree was constructed based on ITS sequences (Figure 7) to explore the phylogenetic relationships among *Cymbidium* species. All *Cymbidium* species were classified into five primary clusters.

Cluster I comprised 11 species, all belonging to the sect. *Jensoa* of the subgenus *Jensoa*. Cluster II consisted of two species from sect. *Cymbidium* of the subgenus *Cymbidium*. Cluster III was the most complex, with 13 species, including 12 from the subgenus *Cyperorchis* (1 species from sect. *Parishiella*, 1 from sect. *Cyperorchis*, 2 from sect. *Eburnea*, and 8 from sect. *Iridorchis*), and 1 from the subgenus *Cymbidium* (*C. dayanum* from sect. *Himentophyllum*). *Cymbidium lancifolium* is a species from the sect. *Geocymbidium* of the subgenus *Jensoa* was grouped into Cluster IV. Two species (*C. floribundum* and *C. suavissimum*) from the same sect. *Floribunda* of the subgenus *Cymbidium* were distinct from all other *Cymbidium* species and formed a separate Cluster V (Figure 7).

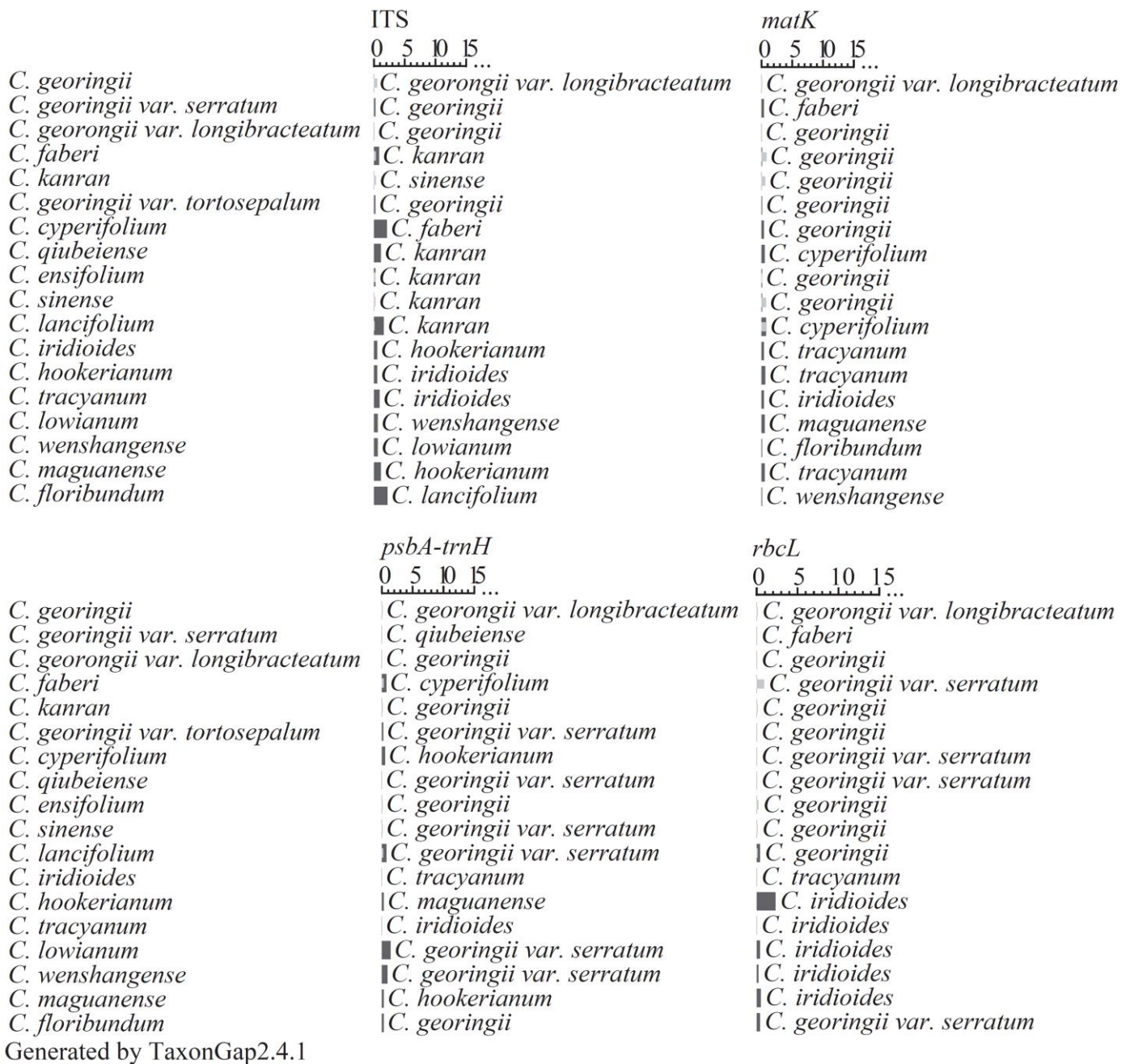
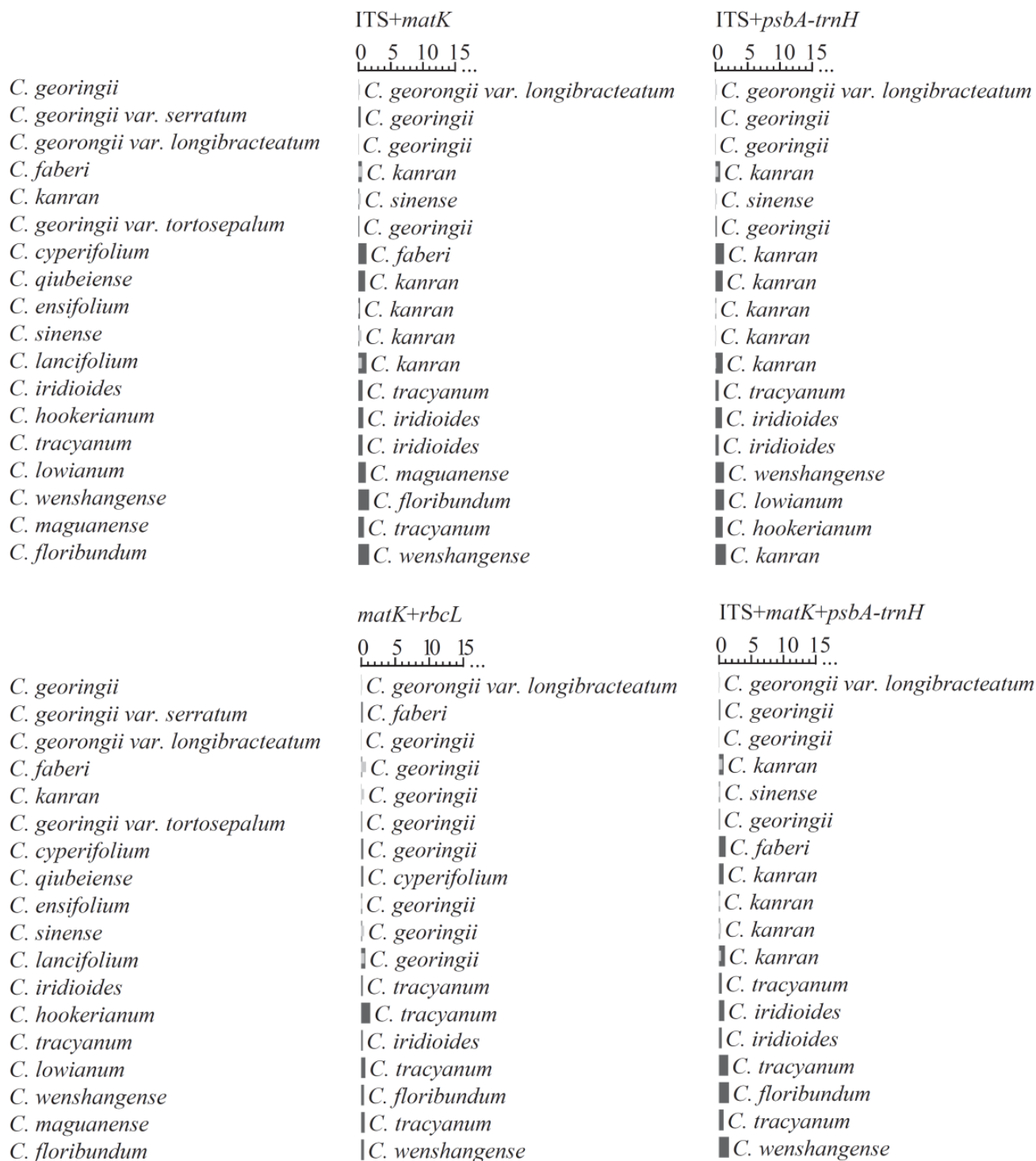


Figure 4. Species identification capability of four loci sequences of 18 *Cymbidium* species using TaxonGap. The complete list of species utilized in this study is presented in the left panel. In the right panel, the horizontal light grey and dark grey bars illustrate the within-species diversity and between-species distinguishability, respectively. Additionally, the right panel displays the names of the most closely related species identified using a similarity-based approach.



Generated by TaxonGap2.4.1

Figure 5. Species identification capability of four regional combinations of 18 *Cymbidium* species using TaxonGap. The complete list of species utilized in this study is presented in the left panel. In the right panel, the horizontal light grey and dark grey bars illustrate the within-species diversity and between-species distinguishability, respectively. Additionally, the right panel displays the names of the most closely related species identified using a similarity-based approach.

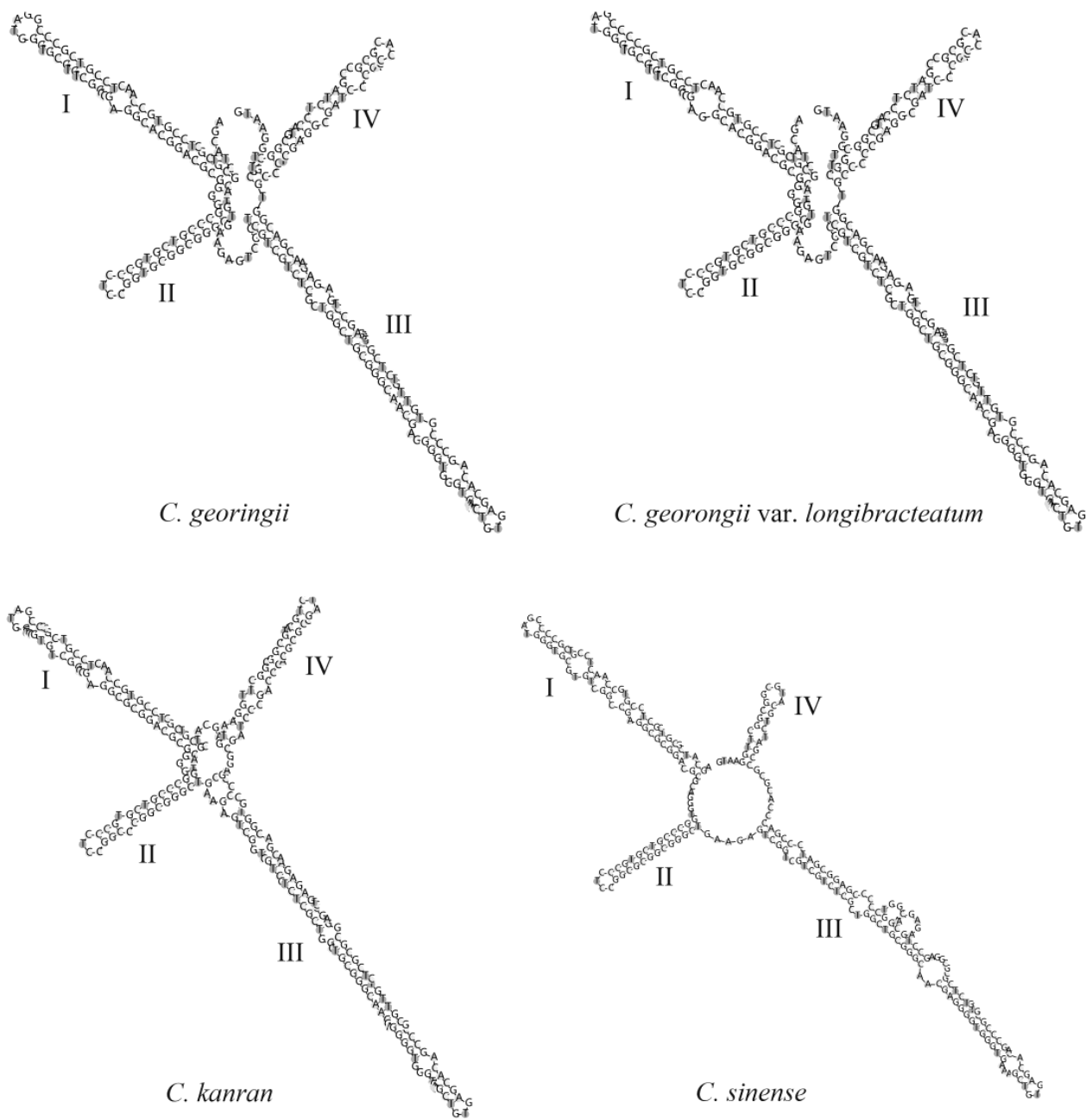


Figure 6. Secondary structures of ITS2 region within ITS sequence of four *Cymbidium* species. The stem-loop domains are labeled as I–IV, and bulges can be seen on each of them.

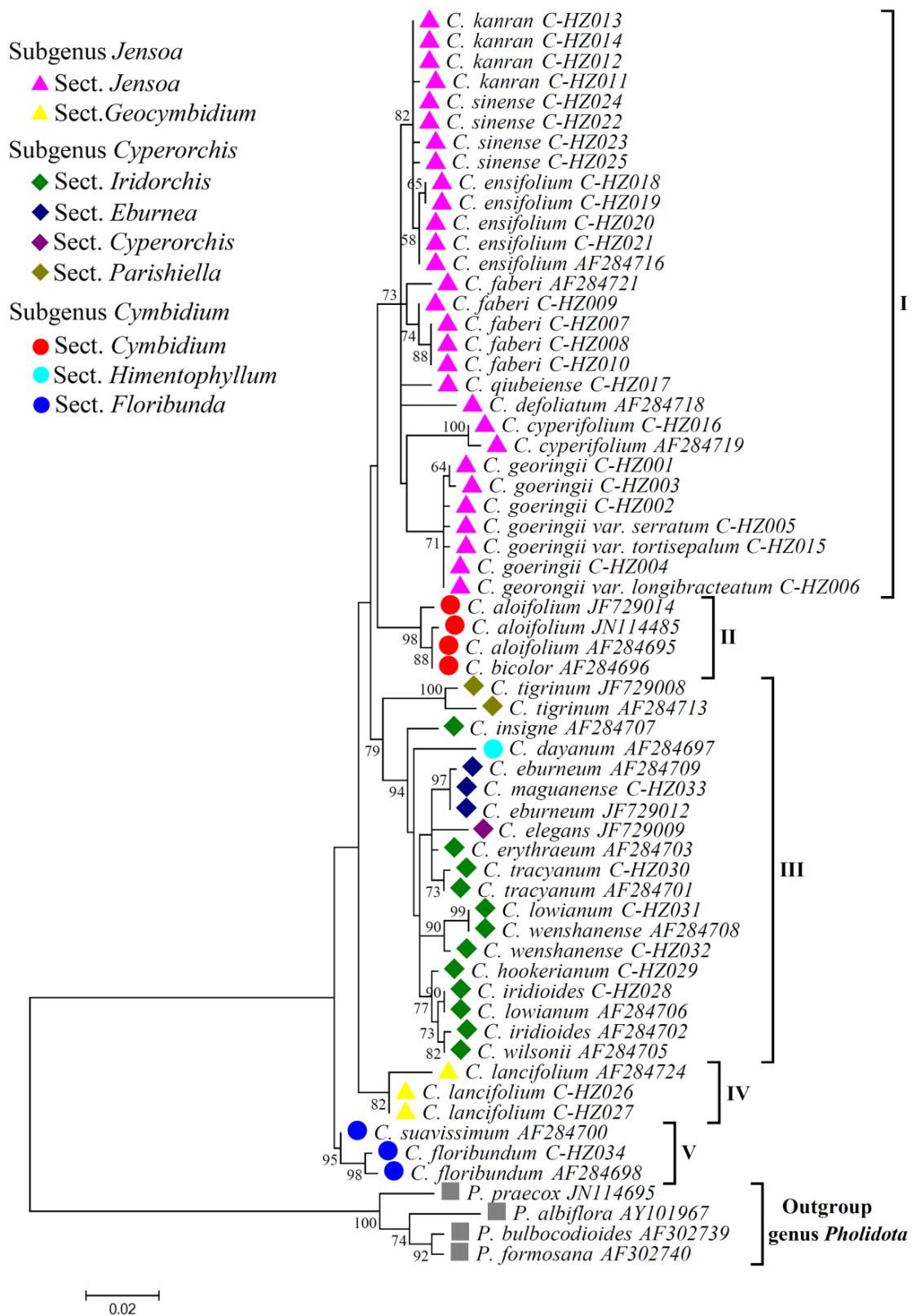


Figure 7. Maximum likelihood (ML) tree based on ITS sequences for *Cymbidium* species collected in this study. Numbers above branches indicate bootstrap (BS \geq 50) values. The ML analysis was performed using the MEGA 7 program under the Tamura-Nei model and assessed by 1000 bootstrapping replicates. All *Cymbidium* species were classified into five primary clusters: I–V.

4. Discussion

The ideal DNA barcodes should exhibit high interspecific variation and low intraspecific variation in order to achieve interspecific discrimination [21,37]. The disparity between intraspecific and interspecific values was termed as the 'barcode gap' [41]. As reported in a previous study [42], we encountered difficulty in directly sequencing the *atpF-atpH* region using PCR. Currently, the chloroplast genomes of certain *Cymbidium* species have been sequenced [1,43,44]. The primers for the *atpF-atpH* region can be redeveloped using this chloroplast genome information, which is expected to enhance and improve the sequencing success rate of this region. Many studies have shown that *rbcL* exhibits very low interspecific variation [42,45]. Our findings indicated that *rbcL* exhibited the lowest interspecific variance and species identification efficiency compared to the other four DNA regions, making it unsuitable for the DNA barcoding of *Cymbidium* species. The *matK* locus was recommended as a core plant barcode by the CBOL plant working group. However, it exhibited a significant overlap, and its success rate in discriminating between species was only 75.8% in our study. Previous research has indicated that *psbA-trnH* could serve as a promising plant barcode [21,41,46,47]. Our findings revealed that the interspecific variation in the *psbA-trnH* region exceeded that of other examined regions within the chloroplast genome. Despite some limitations in using the ITS sequence as a universal barcode [48,49], we found that the ITS possessed the highest interspecific divergence and species resolution rate (93.2%) compared with all plastid regions in our study (Table 2).

Multi-locus combinations may be more preferable than using a single locus for species discrimination [20,48,50]. We found that the species identification rates were significantly higher when using combinations of ITS + *matK*, ITS + *psbA-trnH*, and ITS + *matK* + *psbA-trnH* compared to the investigated plastid regions. However, the results also showed that not all combinations outperformed the ITS region in identifying the tested samples. Notably, the species resolution rate of the *matK* + *rbcL* combination was only 67.0% (Table 2), despite being suggested as a plant barcode by the CBOL plant working group. In fact, several previous studies have reported that combinations of multiple loci are not superior to a single one locus alone for species identification [21,42,51]. Thus, ITS was the best choice for barcoding *Cymbidium* species from the candidate barcode sequences. The variable ITS region based on nuclear DNA provides far more information than certain candidate chloroplast DNA barcode sequences, such as *trnH-psbA*, *matK*, and *rbcL* [52,53]. However, the ITS sequence is not always sufficient for resolving all species identification issues in *Cymbidium*, such as differentiating between *C. georingii* and *C. georingii* var. *longibracteatum* as well as between *C. kanran* and *C. sinense* (Figures 4 and 5). The ITS2 region in the ITS sequence displays significant variability in its sequence, while maintaining a conserved core secondary structure. It also demonstrates similar effectiveness in distinguishing closely related species [54]. Our findings indicated that *C. georingii*, *C. georingii* var. *longibracteatum*, *C. kanran*, and *C. sinense* were distinguishable using the ITS2 secondary structure (Figure 6).

The ITS region proved to be valuable not only for the identification of *Cymbidium* but also as a significant phylogenetic marker. The taxonomy of *Cymbidium* presents a particularly complex puzzle within the Orchidaceae family, as noted in previous studies [1,27,31,33,34]. Our study also revealed a complex taxonomy of the infrageneric taxa of *Cymbidium*. Zhang et al. (2021) also identified inconsistencies between their findings and the conventional categorization of subgenera and sections within *Cymbidium* [35]. At the section level, *Jensoa*, *Cymbidium*, *Parishiella*, *Floribunda*, and *Geocymbidium* were well supported as monophyletic (Figure 7). Species from these sections were grouped into Clusters I (BS = 73), II (BS = 98), III (BS = 100), IV (BS = 82), and V (BS = 95). However, some of the currently defined infrageneric taxa of *Cymbidium* are polyphyletic. For example, the taxonomic status of sect. *Iridorchis*, *Himentophyllum*, *Eburnea*, and *Cyperorchis* requires reassessment and redefinition. However, the samples of sect. *Himentophyllum* and *Cyperorchis* are rarely collected, making it difficult to accurately assess their classification issues. As a type of section of *Cymbidium*, the delimitation of sect. *Iridorchis* has nomenclatural implications for the entire infrageneric system. Van den Berg et al. reported that sect. *Iridorchis* is not monophyletic [30], and

Sharma et al. also argued that the currently defined sect. *Iridorchis* is paraphyletic [31]. Our results indicated that sect. *Iridorchis* was paraphyletic, and some species belonged to several other sections, such as sect. *Himentophyllum*, *Eburnea*, and *Cyperorchis* which were grouped in separate subclades within Cluster III.

At the subgenus level, our results showed that the subgenus *Cyperorchis* was well supported as monophyletic, and all species within this subgenus were grouped into Cluster III. In our study, the subgenus *Jensoa* was mostly monophyletic, as previously reported [33]. This shows that all species from the subgenus *Jensoa*, except *C. lancifolium* (sect. *Geocymbidium*), were grouped into Cluster I. Compared to the subgenera *Cyperorchis* and *Jensoa*, subgenus *Cymbidium* exhibited more intricacies, with species such as *C. aloifolium* and *C. bicolor* from sect. *Cymbidium* included in Cluster II; *C. floribundum* and *C. suavissimum* from sect. *Floribunda* were grouped into Cluster V; and the species belonging to sect. *Himentophyllum* (*C. dayanum*) was grouped into Cluster III along with other species from the subgenus *Cyperorchis*. Hence, it is more favorable to employ a comprehensive and general notion of *Cymbidium* for the purpose of refining the infrageneric classification at the subgenus level, specifically in relation to subgenus *Cymbidium*. Because the *Geocymbidium* and *Floribunda* sections were distant from any other *Cymbidium* species and constituted the separate Clusters IV and V, respectively, we suggest creating two new subgenera for these species.

5. Conclusions

Four plastid loci (*matK*, *rbcL*, *psbA-trnH*, and *atpF-atpH*) and a nuclear locus (ITS) were examined to barcode *Cymbidium* species. The ITS region exhibited a significant difference in genetic distances between inter- and intraspecific variations, and its barcoding gap was more pronounced compared to plastid regions and the four regional combinations studied. Therefore, the ITS region can serve as a reliable barcode for the identification of *Cymbidium* species. Cluster analysis has presented compelling evidence for the potential of the ITS region in contributing to the phylogenetic investigation of the genus *Cymbidium*.

Supplementary Materials: The following supporting information can be downloaded at <https://www.mdpi.com/article/10.3390/agronomy14050933/s1>, Table S1: Sampled *Cymbidium* species and their voucher information used in this study. Voucher samples were deposited in the Zhejiang Provincial Key Laboratory for Genetic Improvement and Quality Control of Medicinal Plants, Hangzhou Normal University, China. Table S2: GenBank accession numbers of the four loci sequences for *Cymbidium* species examined in this study. Table S3: Accession numbers of the ITS sequences of *Cymbidium* species from GenBank.

Author Contributions: S.F. conceived and designed the experiments, participated in the analysis, and drafted the manuscript. Z.C. and L.G. performed the experiments and statistical analysis. S.F. and H.W. collected the plant samples and revised the paper. All authors have read and agreed to the published version of the manuscript.

Funding: This study was supported in part by the National Natural Science Foundation of China (31970346); the Zhejiang Provincial Natural Science Foundation of China (LY20H280012); and the Zhejiang Provincial Key Research & Development Project Grants (2018C02030).

Data Availability Statement: The datasets presented in this study can be found in online repositories. The names of the repository/repositories and accession numbers can be found in the article/Supplementary Materials.

Acknowledgments: Thanks to the staff of the Hangzhou Key Laboratory for Systems Biology of Medicinal and Ornamental Plants, Hangzhou Normal University, for helping to manage and collect experimental materials. Thanks to Guanzhou Chen (NorthCross Shanghai School, Shanghai 200436, China) for his assistance in the data analysis of this study.

Conflicts of Interest: The authors declare no conflicts of interest.

References

1. Yang, J.B.; Tang, M.; Li, H.T.; Zhang, Z.R.; Li, D.Z. Complete chloroplast genome of the genus *Cymbidium*: Lights into the species identification, phylogenetic implications and population genetic analyses. *BMC Evol. Biol.* **2013**, *13*, 84. [[CrossRef](#)] [[PubMed](#)]
2. Yang, F.X.; Gao, J.; Wei, Y.L.; Ren, R.; Zhang, G.Q.; Lu, C.Q.; Jin, J.P.; Ai, Y.; Wang, Y.Q.; Chen, L.J.; et al. The genome of *Cymbidium sinense* revealed the evolution of orchid traits. *Plant Biotechnol. J.* **2021**, *19*, 2501–2516. [[CrossRef](#)] [[PubMed](#)]
3. Kim, H.T.; Chase, M.W. Independent degradation in genes of the plastid *ndh* gene family in species of the orchid genus *Cymbidium* (Orchidaceae; Epidendroideae). *PLoS ONE* **2017**, *12*, e0187318. [[CrossRef](#)] [[PubMed](#)]
4. Sharma, S.K.; Rajkumari, K.; Kumaria, S.; Tandon, P.; Rao, S.R. Karyo-morphological characterization of natural genetic variation in some threatened *Cymbidium* species of Northeast India. *Caryologia* **2010**, *63*, 99–105. [[CrossRef](#)]
5. Yukawa, T.; Stern, W.L. Comparative vegetative anatomy and systematics of *Cymbidium* (Cymbidieae: Orchidaceae). *Bot. J. Linn. Soc.* **2002**, *138*, 383–419. [[CrossRef](#)]
6. Schlechter, R. Die Gattungen *Cymbidium* Sw. und *Cyperorchis* Bl. *Repert. Sp. Nov. Regni.* **1924**, *20*, e96–e110. [[CrossRef](#)]
7. Hunt, P.F. Notes on Asiatic orchis 5. *Kew Bull.* **1970**, *24*, e93–e94. [[CrossRef](#)]
8. Seth, C.J.; Cribb, P.J. A reassessment of the sectional limits in the genus *Cymbidium* Swartz. In *Orchid Biology, Reviews and Prospectives 3*; Cornell University Press: Ithaca, NY, USA; London, UK, 1984.
9. Puy, D.D.; Cribb, P. *The Genus Cymbidium*; Helm, C., Ed.; The University of Chicago Press: Chicago, IL, USA, 1988.
10. Liu, Z.J.; Chen, X.Q.; Ru, Z.Z. *The Genus Cymbidium in China*; Science Press: Beijing, China, 2006.
11. Wang, H.Z.; Wu, Z.X.; Lu, J.J.; Shi, N.N.; Zhao, Y.; Zhang, Z.T.; Liu, J.J. Molecular diversity and relationships among *Cymbidium goeringii* cultivars based on inter-simple sequence repeat (ISSR) markers. *Genetica* **2009**, *136*, 391–399. [[CrossRef](#)]
12. Chen, J.; Chen, M.K.; Zheng, Q.D.; Ma, S.H.; Liu, Z.J.; Ai, Y. Chloroplast characterization and phylogenetic relationship of *Cymbidium aloifolium* (Orchidaceae). *Mitochondrial. DNA B Resour.* **2020**, *5*, 478–479. [[CrossRef](#)]
13. Hollingsworth, P.M. Refining the DNA barcode for land plants. *Proc. Natl. Acad. Sci. USA* **2011**, *108*, 19451–19452. [[CrossRef](#)]
14. Li, D.Z.; Gao, L.M.; Li, H.T.; Wang, H.; Ge, X.J.; Liu, J.Q.; Chen, Z.D.; Zhou, S.L.; Chen, S.L.; Yang, J.B.; et al. Comparative analysis of a large dataset indicates that internal transcribed spacer (ITS) should be incorporated into the core barcode for seed plants. *Proc. Natl. Acad. Sci. USA* **2011**, *108*, 19641–19646.
15. Schindel, D.E.; Miller, S.E. DNA barcoding a useful tool for taxonomists. *Nature* **2005**, *435*, 17. [[CrossRef](#)]
16. Zhang, Z.H.; Jin, Y.Y.; Gao, Y.D.; Zhang, Y.; Ying, Q.C.; Shen, C.J.; Lu, J.J.; Zhan, X.R.; Wang, H.Z.; Feng, S.G. The Complete chloroplast genomes of two *Physalis* species, *Physalis macrophysa* and *P. ixocarpa*: Comparative genomics, evolutionary dynamics and phylogenetic relationships. *Agronomy* **2023**, *13*, 135. [[CrossRef](#)]
17. Bergmann, T.; Rach, J.; Damm, S.; Desalle, R.; Schierwater, B.; Hadrys, H. The potential of distance-based thresholds and character-based DNA barcoding for defining problematic taxonomic entities by *CO1* and *ND1*. *Mol. Ecol. Resour.* **2013**, *13*, 1069–1081. [[CrossRef](#)]
18. Karamat, S.; Ashraf, N.; Akhtar, T.; Rahim, F.; Shafi, N.; Khalid, S.; Shahid, B.; Khawaja, S.; Rahim, J.; Majeed, Z.; et al. *CO1*-Based DNA barcoding for assessing diversity of *Pteropus giganteus* from the state of Azad Jammu Kashmir, Pakistan. *Braz. J. Biol.* **2021**, *81*, 584–591. [[CrossRef](#)]
19. Larranaga, N.; Hormaza, J.I. DNA barcoding of perennial fruit tree species of agronomic interest in the genus *Annona* (Annonaceae). *Front. Plant Sci.* **2015**, *6*, 589. [[CrossRef](#)] [[PubMed](#)]
20. Cbol Plant Working Group. A DNA barcode for land plants. *Proc. Natl. Acad. Sci. USA* **2009**, *106*, 12794–12797. [[CrossRef](#)]
21. Chen, S.L.; Yao, H.; Han, J.P.; Liu, C.; Song, J.Y.; Shi, L.C.; Zhu, Y.J.; Ma, X.Y.; Gao, T.; Pang, X.H.; et al. Validation of the ITS2 region as a novel DNA barcode for identifying medicinal plant species. *PLoS ONE* **2010**, *5*, e8613. [[CrossRef](#)] [[PubMed](#)]
22. Li, X.W.; Yang, Y.; Henry, R.J.; Rossetto, M.; Wang, Y.T.; Chen, S.L. Plant DNA barcoding: From gene to genome. *Biol. Rev. Camb. Philos. Soc.* **2015**, *90*, 157–166. [[CrossRef](#)] [[PubMed](#)]
23. Xiong, C.; Sun, W.; Wu, L.; Xu, R.; Zhang, Y.; Zhu, W.; Panjwani; Liu, Z.; Zhao, B. Evaluation of four commonly used DNA barcoding loci for *Ardisia* species identification. *Front. Plant Sci.* **2022**, *13*, 860778. [[CrossRef](#)]
24. Siripiyasing, P.; Kaenratana, K.; Mookamul, P.; Tanee, T.; Sudmoon, R.; Chaveerach, A. DNA barcoding of the *Cymbidium* species (Orchidaceae) in Thailand. *Afr. J. Agric. Res.* **2012**, *7*, 393–404.
25. Obara-Okeyo, P.; Kako, S. Genetic diversity and identification of *Cymbidium* cultivars as measured by random amplified polymorphic DNA (RAPD) markers. *Euphytica* **1998**, *99*, 95–101. [[CrossRef](#)]
26. Wang, H.Z.; Wang, Y.D.; Zhou, X.Y.; Ying, Q.C.; Zheng, K.L. Analysis of genetic diversity of 14 species of *Cymbidium* based on RAPDs and AFLPs. *Shi Yan Sheng Wu Xue Bao* **2004**, *37*, 482–486. [[PubMed](#)]
27. Wu, Z.X.; Wang, H.Z.; Shi, N.N.; Zhao, Y. The genetic diversity of *Cymbidium* by ISSR. *Yi Chuan* **2008**, *30*, 627–632. [[CrossRef](#)] [[PubMed](#)]
28. Sharma, S.K.; Kumaria, S.; Tandon, P.; Rao, S.R. Assessment of genetic variation and identification of species-specific ISSR markers in five species of *Cymbidium* (Orchidaceae). *J. Plant Biochem. Biot.* **2013**, *22*, 250–255. [[CrossRef](#)]
29. Moe, K.T.; Zhao, W.; Song, H.S.; Kim, Y.H.; Chung, J.W.; Cho, Y.I.; Park, P.H.; Park, H.S.; Chae, S.C.; Park, Y.J. Development of SSR markers to study diversity in the genus *Cymbidium*. *Biochem. Syst. Ecol.* **2010**, *38*, 585–594. [[CrossRef](#)]
30. Van den Berg, C.; Ryan, A.; Cribb, P.; Chase, M. Molecular phylogenetics of *Cymbidium* (Orchidaceae: Maxillarieae) sequence data from internal transcribed spacers (ITS) of nuclear ribosomal DNA and plastid *matK*. *Lindleyana* **2002**, *17*, 102–111.

31. Sharma, S.K.; Dkhar, J.; Kumaria, S.; Tandon, P.; Rao, S.R. Assessment of phylogenetic inter-relationships in the genus *Cymbidium* (Orchidaceae) based on internal transcribed spacer region of rDNA. *Gene* **2012**, *495*, 10–15. [[CrossRef](#)]
32. Zhang, L.; Huang, Y.W.; Huang, J.L.; Ya, J.D.; Zhe, M.Q.; Zeng, C.X.; Zhang, Z.R.; Zhang, S.B.; Li, D.Z.; Li, H.T.; et al. DNA barcoding of *Cymbidium* by genome skimming: Call for next-generation nuclear barcodes. *Mol. Ecol. Resour.* **2022**, *23*, 424–439. [[CrossRef](#)]
33. Wang, X.M.; Cheng, L.J.; Li, Z.L.; Zhang, Z.C.; Wang, Y.Y. Characterization of the complete chloroplast genome of a Chinese endangered species *Cymbidium wenshanense* Y. S. Wu et F. Y. Liu. *Mitochondrial. DNA B Resour.* **2023**, *8*, 815–818. [[CrossRef](#)]
34. Choi, S.; Kim, M.; Lee, J.; Ryu, K. Genetic diversity and phylogenetic relationships among and within species of oriental *Cymbidiums* based on RAPD analysis. *Sci. Hortic.* **2006**, *108*, 79–85. [[CrossRef](#)]
35. Zhang, G.Q.; Chen, G.Z.; Chen, L.J.; Zhai, J.W.; Huang, J.; Wu, X.Y.; Li, M.H.; Peng, D.H.; Rao, W.H.; Liu, Z.J.; et al. Phylogenetic incongruence in *Cymbidium* orchids. *Plant Divers.* **2021**, *43*, 452–461. [[CrossRef](#)]
36. Thompson, J.D.; Gibson, T.J.; Higgins, D.G. Multiple Sequence Alignment Using ClustalW and ClustalX. *Curr. Protoc. Bioinform.* **2002**, *1*, 2–3. [[CrossRef](#)]
37. Kumar, S.; Stecher, G.; Tamura, K. MEGA7: Molecular Evolutionary Genetics Analysis Version 7.0 for Bigger Datasets. *Mol. Biol. Evol.* **2016**, *33*, 1870–1874. [[CrossRef](#)]
38. Feng, S.G.; Jiang, M.Y.; Shi, Y.J.; Jiao, K.L.; Shen, C.J.; Lu, J.J.; Ying, Q.C.; Wang, H.Z. Application of the ribosomal DNA ITS2 region of *Physalis* (Solanaceae): DNA barcoding and phylogenetic study. *Front. Plant Sci.* **2016**, *7*, 1047. [[CrossRef](#)]
39. Slabbinck, B.; Dawyndt, P.; Martens, M.; De Vos, P.; De Baets, B. TaxonGap: A visualization tool for intra- and inter-species variation among individual biomarkers. *Bioinformatics* **2008**, *24*, 866–867. [[CrossRef](#)]
40. Chinese Academy of Sciences. *Flora of China*; Science Press: Beijing, China, 1999; Volume 18, p. 191.
41. Lahaye, R.; Van der Bank, M.; Bogarin, D.; Warner, J.; Pupulin, F.; Gigot, G.; Maurin, O.; Duthoit, S.; Barraclough, T.G.; Savolainen, V. DNA barcoding the floras of biodiversity hotspots. *Proc. Natl. Acad. Sci. USA* **2008**, *105*, 2923–2928. [[CrossRef](#)]
42. Xiang, X.G.; Hu, H.; Wang, W.; Jin, X.H. DNA barcoding of the recently evolved genus *Holcoglossum* (Orchidaceae: Aeridinae): A test of DNA barcode candidates. *Mol. Ecol. Resour.* **2011**, *11*, 1012–1021. [[CrossRef](#)]
43. Wang, Y.Y.; Cheng, L.J.; Zhao, Y.R.; Li, Y.F.; He, F.M.; Li, Z.L. Characterization of the complete chloroplast genome of a Chinese endangered species *Cymbidium mannii*. *Mitochondrial. DNA B Resour.* **2020**, *5*, 3199–3200. [[CrossRef](#)]
44. Du, Z.H.; Yang, X.Y.; Tan, G.F.; Chen, Z.L. The complete chloroplast genome of *Cymbidium dayanum* (Orchidaceae). *Mitochondrial. DNA B Resour.* **2021**, *6*, 1897–1898. [[CrossRef](#)]
45. Newmaster, S.G.; Fazekas, A.J.; Steeves, R.A.; Janovec, J. Testing candidate plant barcode regions in the Myristicaceae. *Mol. Ecol. Resour.* **2008**, *8*, 480–490. [[CrossRef](#)] [[PubMed](#)]
46. Feng, S.G.; Jiao, K.L.; Zhu, Y.J.; Wang, H.H.; Jiang, M.Y.; Wang, H.Z. Molecular identification of species of *Physalis* (Solanaceae) using a candidate DNA barcode: The chloroplast *psbA-trnH* intergenic region. *Genome* **2018**, *61*, 15–20. [[CrossRef](#)]
47. Fujii, T.; Mori, T.; Tatsuo, Y.; Takao, Y.; Fujino, H.; Tsuchida, T.; Minami, M. Identification of *Valeriana fauriei* and other Eurasian medicinal valerian by DNA polymorphisms in *psbA-trnH* intergenic spacer sequences in chloroplast DNA. *J. Nat. Med.* **2021**, *75*, 699–706. [[CrossRef](#)] [[PubMed](#)]
48. Kress, W.J.; Erickson, D.L. A two-locus global DNA barcode for land plants: The coding *rbcl* gene complements the non-coding *trnH-psbA* spacer region. *PLoS ONE* **2007**, *2*, e508. [[CrossRef](#)] [[PubMed](#)]
49. Sass, C.; Little, D.P.; Stevenson, D.W.; Specht, C.D. DNA barcoding in the cycadales: Testing the potential of proposed barcoding markers for species identification of cycads. *PLoS ONE* **2007**, *2*, e1154. [[CrossRef](#)]
50. Newmaster, S.; Fazekas, A.; Ragupathy, S. DNA barcoding in land plants: Evaluation of *rbcl* in a multigene tiered approach. *Botany* **2006**, *84*, 335–341. [[CrossRef](#)]
51. Starr, J.R.; Naczi, R.F.; Chouinard, B.N. Plant DNA barcodes and species resolution in sedges (Carex, Cyperaceae). *Mol. Ecol. Resour.* **2009**, *9* (Suppl. S1), 151–163. [[CrossRef](#)]
52. Gao, T.; Yao, H.; Song, J.Y.; Zhu, Y.J.; Liu, C.; Chen, S.L. Evaluating the feasibility of using candidate DNA barcodes in discriminating species of the large Asteraceae family. *BMC Evol. Biol.* **2010**, *10*, 324. [[CrossRef](#)] [[PubMed](#)]
53. Thomas, C. *Plant Bar Code Soon to Become Reality*; Science: New York, NY, USA, 2009; Volume 325, p. 526.
54. Samanta, B.; Ehrman, J.M.; Kaczmarska, I. A consensus secondary structure of ITS2 for the diatom Order Cymatosirales (Mediophyceae, Bacillariophyta) and reappraisal of the order based on DNA, morphology, and reproduction. *Mol. Phylogenet. Evol.* **2018**, *129*, 117–129. [[CrossRef](#)]

Disclaimer/Publisher's Note: The statements, opinions and data contained in all publications are solely those of the individual author(s) and contributor(s) and not of MDPI and/or the editor(s). MDPI and/or the editor(s) disclaim responsibility for any injury to people or property resulting from any ideas, methods, instructions or products referred to in the content.